

W. Liu | R. Tkachov | H. Komber | V. Senkovskyy | M. Schubert  
Z. Wei | A. Facchetti | D. Neher | A. Kiriy

# Chain-growth polycondensation of perylene diimide-based copolymers

a new route to regio-regular perylene diimide-based acceptors for all-polymer solar cells and n-type transistors

Suggested citation referring to the original publication:

Polym. Chem. 5, 2014, pp. 3404–3411

DOI <http://dx.doi.org/10.1039/C3PY01707A>

ISSN (online) 1759-9962

ISSN (print) 1759-9954

Postprint archived at the Institutional Repository of the Potsdam University in:

Postprints der Universität Potsdam

Mathematisch-Naturwissenschaftliche Reihe ; 273

ISSN 1866-8372

<http://nbn-resolving.de/urn:nbn:de:kobv:517-opus4-98724>



# Chain-growth polycondensation of perylene diimide-based copolymers: a new route to regio-regular perylene diimide-based acceptors for all-polymer solar cells and n-type transistors†

Cite this: *Polym. Chem.*, 2014, 5, 3404W. Liu,<sup>a</sup> R. Tkachov,<sup>a</sup> H. Komber,<sup>a</sup> V. Senkovskyy,<sup>b</sup> M. Schubert,<sup>c</sup> Z. Wei,<sup>d</sup> A. Facchetti,<sup>\*d</sup> D. Neher<sup>c</sup> and A. Kiriy<sup>\*a</sup>

Herein, we report the chain-growth tin-free room temperature polymerization method to synthesize n-type perylene diimide-dithiophene-based conjugated polymers (PPDIT2s) suitable for solar cell and transistor applications. The palladium/electron-rich tri-*tert*-butylphosphine catalyst is effective to enable the chain-growth polymerization of anion-radical monomer Br-TPDIT-Br/Zn to PPDIT2 with a molecular weight up to  $M_w \approx 50 \text{ kg mol}^{-1}$  and moderate polydispersity. This is the second example of the polymerization of unusual anion-radical aromatic complexes formed in a reaction of active Zn and electron-deficient diimide-based aryl halides. As such, the discovered polymerization method is not a specific reactivity feature of the naphthalene-diimide derivatives but is rather a general polymerization tool. This is an important finding, given the significantly higher maximum external quantum efficiency that can be reached with PDI-based copolymers (32–45%) in all-polymer solar cells compared to NDI-based materials (15–30%). Our studies revealed that PPDIT2 synthesized by the new method and the previously published polymer prepared by step-growth Stille polycondensation show similar electron mobility and all-polymer solar cell performance. At the same time, the polymerization reported herein has several technological advantages as it proceeds relatively fast at room temperature and does not involve toxic tin-based compounds. Because several chain-growth polymerization reactions are well-suited for the preparation of well-defined multi-functional polymer architectures, the next target is to explore the utility of the discovered polymerization in the synthesis of end-functionalized polymers and block copolymers. Such materials would be helpful to improve the nanoscale morphology of polymer blends in all-polymer solar cells.

Received 12th December 2013  
Accepted 25th January 2014

DOI: 10.1039/c3py01707a

[www.rsc.org/polymers](http://www.rsc.org/polymers)

## Introduction

N-type (or electron-conducting) polymers are essential components for organic devices such as ambipolar and n-channel field-effect transistors and organic photovoltaics.<sup>1</sup> Perylene diimide (PDI) alternating main chain copolymers are an intriguing class of electron-conducting materials with excellent charge transport properties.<sup>2</sup> Furthermore, PDI-containing copolymers show a widely tunable optical bandgap and relatively high electron affinities (low LUMO energies), which make them

well-suited to be used as the electron accepting component in organic solar cells.<sup>3</sup> Recently, Hashimoto *et al.* reported the synthesis of several PDI copolymers.<sup>4</sup> In combination with a polythiophene donor polymer, a power conversion efficiency (PCE) of above 2% was reached. Despite considerable progress in the field of all-polymer solar cells,<sup>5,6</sup> their efficiency remains significantly lower than the efficiency of fullerene-based solar cells.<sup>7</sup> Several intrinsic factors, such as lower polarizability, symmetry and dielectric constant of polymers relative to fullerenes, may explain the lower performance. Yi and coworkers demonstrated the strong influence of the shape of the acceptor molecule on the processes at the donor–acceptor interface governing charge separation, which revealed a faster geminate recombination of PDI compared to fullerene C<sub>60</sub>.<sup>8</sup> In addition, a higher tendency for large scale phase separation is expected for all-polymer blends due to their small entropy of mixing.<sup>9</sup> For these reasons, control of the blend morphology and donor–acceptor interface – factors always important in fullerene-based solar cells – becomes even more crucial in

<sup>a</sup>Leibniz-Institut für Polymerforschung Dresden e.V. Hohe Straße 6, 01069 Dresden, Germany. E-mail: kiriy@ipfdd.de

<sup>b</sup>NOVALED AG, Tatzberg 49, 01307 Dresden, Germany

<sup>c</sup>Institute of Physics and Astronomy, University of Potsdam, Karl-Liebknecht-Str. 24-25, 14476 Potsdam, Germany

<sup>d</sup>Polyera Corporation, 8045 Lamon Avenue, Skokie, Illinois 60077, USA. E-mail: a-facchetti@northwestern.edu

† Electronic supplementary information (ESI) available: Monomer preparation procedure. See DOI: 10.1039/c3py01707a

all-polymer solar cells.<sup>5,10</sup> It is believed that advanced architectures of conjugated polymers such as well-defined conjugated block copolymers, brushes and end-functionalized conjugated polymers are promising materials for heterojunction devices as they might allow better control of the domain structure and film morphology as well as controlled modification of the heterojunction.<sup>11</sup>

With respect to the synthesis of more complex polymers, conventional step-growth polycondensation reactions are typically used to synthesize perylene diimide-based alternating copolymers.<sup>4,12</sup> Although rather significant progress was achieved over the last few years in the employment of step-growth polymerization reactions in the synthesis of bis-end-functionalized conjugated polymers<sup>13</sup> and A–B–A triblock copolymers,<sup>14</sup> chain-growth polymerization reactions are potentially more straightforward for the preparation of well-defined multi-functional polymer architectures, due to the one by one addition of monomers from defined initiators.<sup>15</sup> Moreover, the often used Stille-polycondensation utilizes highly toxic organostannyl derivatives and requires high temperatures and long reaction times.<sup>16</sup>

Chain-growth catalyst-transfer polycondensation reactions of AB-type monomers are a new and rapidly developing polymerization tool for the preparation of well-defined conjugated homopolymers, gradients and block copolymers.<sup>17–23</sup> Until recently, the scope of chain-growth polycondensation reactions was limited to the preparation of simple, yet electron-rich polymers, such as polythiophenes, polyphenylenes, and polyfluorenes. However, the chain-growth synthesis of donor-acceptor copolymers is much more difficult to implement because of the increased size of the monomers and their complex polarization pattern.<sup>24</sup> These factors impede intramolecular catalyst transfer which is the key for the chain-growth propagation mechanism.<sup>25</sup>

Recently, we discovered unusual Ni-catalyzed polymerization of an anion-radical complex between Zn and 2,6-bis(2-bromothien-5-yl)naphthalene-1,4,5,8-tetracarboxylic-*N,N'*-bis(2-octyldodecyl)diimide (Br-TNDIT-Br).<sup>26,27</sup> Polymerization involved the chain-growth mechanism and yielded the corresponding donor-acceptor alternating copolymer, PNDIT2, with controlled molecular weight, low polydispersity and specific end-functions. It is noteworthy that the high electron-deficiency of NDI-based compounds is provided by imide moieties attached to the aromatic core. On the other hand, several other aryl imides were discovered (*e.g.*, perylene diimides,<sup>4</sup> isoindigos,<sup>28,29</sup> diketopyrrolopyrroles,<sup>30</sup> *etc.*) which are important for optoelectronic applications. In view of this, it is of great interest to study the scope and limitation of the newly discovered polymerization tool and, particularly, to verify its applicability in polymerization of other aryl imides. In the present work we investigate the polymerization of 2,6-bis(2-bromothien-5-yl)perylene-1,4,5,8-tetracarboxylic-*N,N'*-bis(2-octyldodecyl)diimide (Br-TPDIT-Br), the perylene diimide-based analogue of PNDIT2, in the presence of activated Zn and transition metal catalysts. It is, however, worth mentioning that the monomer preparation procedure involves the reaction of a strongly electron-deficient monomer precursor with a strong reducing reagent. Such conditions may, in principle, derive undesirable irreversible

redox side reactions that would potentially affect the structural purity of the resulting PPDIT2 and alter its optoelectronic properties. It was therefore important to evaluate the optoelectronic properties of PPDIT2 achieved by the new method and compare them to the performance of the polymer synthesized by Pd-catalyzed step-growth Stille polycondensation.

## Experimental

### Materials

Active zinc was prepared by the reduction of ZnCl<sub>2</sub> with sodium naphthalenide.<sup>26</sup> Tetrahydrofuran (THF) was distilled over sodium benzophenone ketyl. Synthesis of monomer precursor Br-TPDIT-Br is described in the ESI.† PPDIT2<sub>control</sub> (commercial name ActivInk N2200) was provided by the Polyera Corporation and synthesized following the previously published recipe.<sup>12b</sup> Regio-regular P3HT (Sepiolid P200 from BASF) was purchased from Rieke Metals. All other chemicals for synthesis were purchased from Aldrich and used as received.

### Polymerization

All operations were carried out under argon in a glove box. The charge-transfer monomer was prepared as follows: Br-TPDIT-Br (509 mg, 0.4 mmol) was dissolved in dry THF (60 mL) in a round-bottomed flask equipped with a magnetic stirrer and a septum. The suspension of active Zn (~100 mg, ~1.6 mmol) was added with a syringe and the mixture was stirred at room temperature for 1 h. Then, the solution was filtered through a filter (0.2 mm) to remove an excess of unreacted Zn. Titration of the thus-prepared monomer solution gives 1/1 mole ratio of Br-TPDIT-Br/Zn. Palladium catalyst (1.5 mg, 0.01 equiv.) prepared by mixing of Pd(CH<sub>3</sub>CN)<sub>2</sub>Cl<sub>2</sub> and P<sup>t</sup>Bu<sub>3</sub> (1 equivalent of each) was added to the monomer mixture and stirred for 2 h at room temperature. The polymerization mixture was quenched with methanol (10 mL). The solvent was evaporated and the polymer was washed with methanol, acetone and hexane in a Soxhlet extractor. The resulting PPDIT2 was obtained as a black powder (~350 mg, 78%).

### Thin-film transistors

The top-gate, bottom-contact OTFT devices were fabricated on glass substrates (Precision Glass & Optics, Eagle 2000). The gold source and drain electrodes (~35 nm) were deposited by thermal evaporation using a shadow mask ( $L = 50 \mu\text{m}$ ,  $W = 500 \mu\text{m}$ ). The semiconductor films were spin-coated from PPDIT2 solution in *ortho*-dichlorobenzene, DCB (8 g L<sup>-1</sup>). Then Cytop (Asahi Glass CTL-809M) diluted with CT Solv-180 at the ratio of 3 : 1 was spin-coated at 1500 rpm for 60 s as the dielectric layer. The dielectric film was then baked at 110 °C on a hotplate for 10 min before deposition of a ~35 nm gold thin film as the gate electrode. The measured capacitance of the Cytop dielectric layer is 3.5 nF cm<sup>-2</sup>. The finished devices were tested under ambient conditions.

### Bulk-heterojunction solar cells

Solar cell devices were prepared on cleaned and pre-structured indium tin oxide (ITO)-coated glass substrates. The ZnO precursor solution was prepared as described in the literature<sup>38</sup>

and spin-coated in air at 4000 rpm and dried in air for 20 min at 200 °C. The thickness of the final ZnO layer was 30 nm. Active layers were spin-coated for 5 s at 1400 rpm from hot solutions (80 °C) from either pure DCB or a 1 : 1 Xy : CN (*p*-xylene : 1-chloronaphthalene) solvent mixture. The donor : acceptor (P3HT:PPDIT2) ratio was 1.5 : 1 and the overall concentration was 35 g L<sup>-1</sup> for all blends. Fast dried active layers were prepared following a recently published routine,<sup>34</sup> while slowly dried samples were kept at room temperature in a small Petri dish. Device fabrication was completed by evaporation of a 10 nm molybdenum trioxide layer, capped with 100 nm silver. The final device structure is: glass/ITO/ZnO/blend/MoO<sub>3</sub>/Ag. All preparation and measurement steps were kept under an inert nitrogen atmosphere. The active area of the device was 16 mm<sup>2</sup>. Current–voltage measurements were performed with a Keithley 2400 source-measure unit. For illumination a Newport Oriol Sol2A solar simulator was used, which was calibrated with a KG5 filtered reference silicon solar cell. The intensity was set to 100 mW cm<sup>-2</sup>. For EQE measurements, frequency modulated monochromatic light of a 100 W quartz halogen lamp (Philips 7724) was focused into a Cornerstone 260 1/4m monochromator (model 74100). The setup was calibrated before each measurement by a calibrated Si photodiode from Newport.

## Results and discussion

### Monomer synthesis and polymerization

The synthesis of the monomer precursor Br-TPDIT-Br was initiated by standard bromination of perylene diimide which afforded a mixture of 1,6- and 1,7-regio-isomers (at a mole ratio of approximately 1 : 3, Scheme S1, ESI†). It was previously demonstrated that copolymerization of the mixture of the isomers leads to regioirregular PDI-based polymers which are less attractive for optoelectronic applications than the respective regioregular polymers.<sup>12b</sup> Regioregular PDI-polymers can be synthesized from pure 1,7-dibromide, however, their preparation requires multiple column chromatography steps. In the present work, the crude mixture of dibromo-isomers was subjected to Stille coupling which afforded a mixture of the respective H-TPDIT-H regioisomers. We found that isolation of the pure 1,7-isomer of H-TPDIT-H is easy at this stage and requires a single column chromatography step. A standard bromination with NBS leads to regioregularly pure Br-TPDIT-Br (Fig. 1a and b).

In order to provide the chain-growth catalyst-transfer mechanism, asymmetric AB-type monomers having metal-organic (nucleophilic) and halide (electrophilic) functions in the same molecule must be involved in polycondensation. In the case of electron-rich aryl dihalide precursors, such monomers are commonly prepared by reactions with alkyl magnesium halides or other metalorganic molecules. Although electron-deficient aryl halides are usually more reactive in halogen–metal exchange reactions than their electron-rich counterparts,<sup>31</sup> we found that Br-TPDIT-MgBr does not form upon the reaction of Br-TNDIT-Br with various alkyl magnesium halides. Mixing of Br-TNDIT-Br and *t*-BuMgCl leads to immediate change of color of the reaction mixture suggesting some

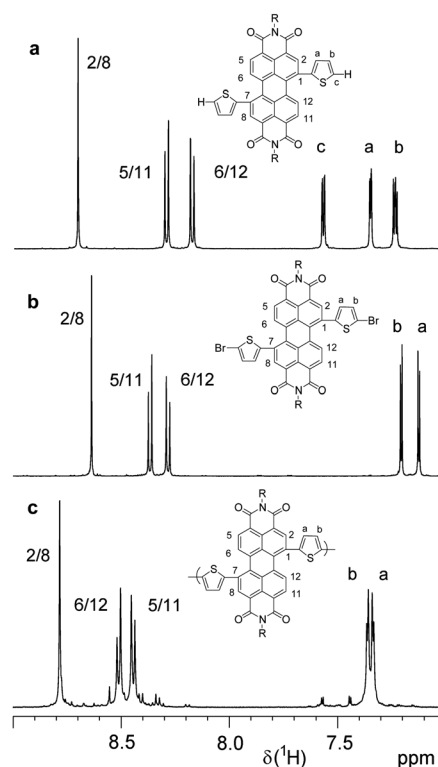
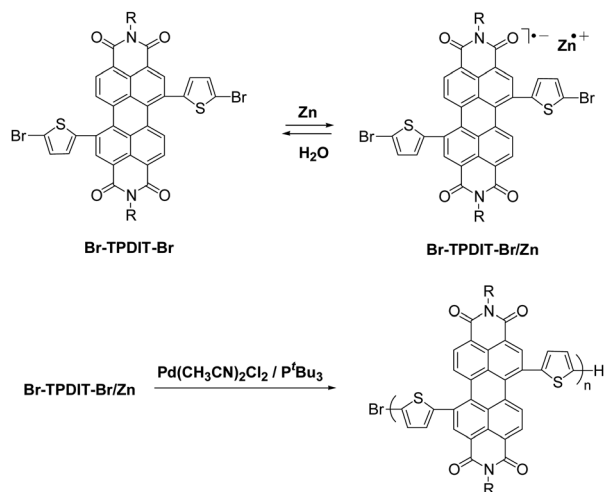


Fig. 1 <sup>1</sup>H NMR spectra (region of aromatic and thiophene protons) of (a) 1,7-H-TPDIT-H, (b) Br-TPDIT-Br and (c) PPDIT2; R = CH<sub>2</sub>CHOct-Dec; solvent: C<sub>2</sub>D<sub>2</sub>Cl<sub>4</sub> at 120 °C.

chemical transformation, however, the process does not lead to the corresponding product Br-TPDIT-MgBr. This follows from the fact that intact Br-TPDIT-Br is quantitatively recovered upon quenching of the reaction mixture with water indicative of the absence of the bromo-magnesium exchange. Similarly, the treatment of Br-TPDIT-Br with *n*-BuLi failed to give the corresponding lithiation product Br-TPDIT-Li. Such behavior was previously observed during attempts of activation of structurally similar naphthalene-diimide derivatives.<sup>26</sup> We explain these results by a concurrent single-electron transfer from electron-rich alkyl metals to electron-deficient dibromo-arylimide which occurs faster than the halogen–metal exchange. The electron-transfer leads, from one side, to decomposition of alkyl metals and, from the other side to deactivation of dibromo-aryl imides, which are transformed into electron-rich anion-radicals inactive in the halogen–metal exchange. It was further found that addition of Ni and Pd catalysts to the mixture of Br-TPDIT-Br and alkyl magnesium halides (or *n*-BuLi) does not induce polymerization. As such, a strong electron-affinity of dibromoaryls containing strongly electron-deficient groups which precludes their transformation into AB-type monomers is an important and general obstacle in development of chain-growth preparation of n-type semiconducting polymers.

Luckily, an alternative route was found in our previous studies to activate the electron-deficient naphthalene-diimide-based dihalide Br-TNDIT-Br.<sup>26</sup> In the present work we demonstrate that this approach is also suitable for activation of Br-TPDIT-Br. Particularly, we found that Br-TPDIT-Br reacts



**Scheme 1** Preparation of the Br-TPDIT-Br/Zn radical-anion monomer and its polymerization.

with activated Zn powder within minutes at room temperature resulting in the Br-TPDIT-Br/Zn complex soluble in THF. Titration experiments with iodine revealed the 1/1 stoichiometry of the Br-TNDIT-Br/Zn complex, irrespective of whether an equimolar amount or an excess of Zn was added. The acidic workup of the Br-TPDIT-Br/Zn complex resulted in quantitative recovering of Br-TPDIT-Br but not of Br-TPDIT-H. This indicates that the organo-zinc compound Br-TPDIT-ZnBr was not formed under these conditions because otherwise hydrolysis of Br-TPDIT-ZnBr should lead to Br-TPDIT-H. Electron spin-resonance measurements of the Br-TNDIT-Br/Zn complex reveal its paramagnetic character (Fig. S1†). Thus, single electron transfer from Zn to electron-deficient Br-TPDIT-Br occurs which leads to Br-TPDIT-Br/Zn having a radical-anion character (Scheme 1). As such, Br-TPDIT-Br and its NDI-based analogues behave similarly in the presence of Zn. However, despite the similarities between the Br-TPDIT-Br/Zn and Br-TNDIT-Br/Zn structures and the fact that Br-TNDIT-Br/Zn smoothly polymerized in the presence of Ni, various Ni catalysts were found to be inactive to polymerize Br-TPDIT-Br/Zn.

It was previously shown that Pd complexes frequently display higher catalytic activity than their Ni counterparts in a variety of cross-coupling reactions of small molecules and related polycondensation reactions.<sup>32</sup> Among several of the ligands employed, bulky and electron-rich tri-*tert*-butylphosphine ( $\text{P}^t\text{Bu}_3$ ) is a promising ligand for Pd to support catalyst-transfer polycondensation reactions.<sup>33</sup> It is because  $\text{P}^t\text{Bu}_3$  efficiently stabilizes highly coordination unsaturated Pd- $\text{P}^t\text{Bu}_3$  species and promotes the preferred intramolecular oxidative addition pathway responsible for the chain-growth behavior over the intermolecular process. Recently, we, in collaboration with the Huck group, employed Pd/ $\text{P}^t\text{Bu}_3$  in chain-growth Suzuki polymerization of a benzothiadiazolo-based donor-acceptor monomer.<sup>24</sup>

The Pd/ $\text{P}^t\text{Bu}_3$ -based catalyst was prepared *in situ* by mixing one equivalent of  $\text{Pd}(\text{CH}_3\text{CN})_2\text{Cl}_2$  and one equivalent of  $\text{P}^t\text{Bu}_3$ . The addition of Br-TPDIT-Br/Zn to the freshly prepared catalyst

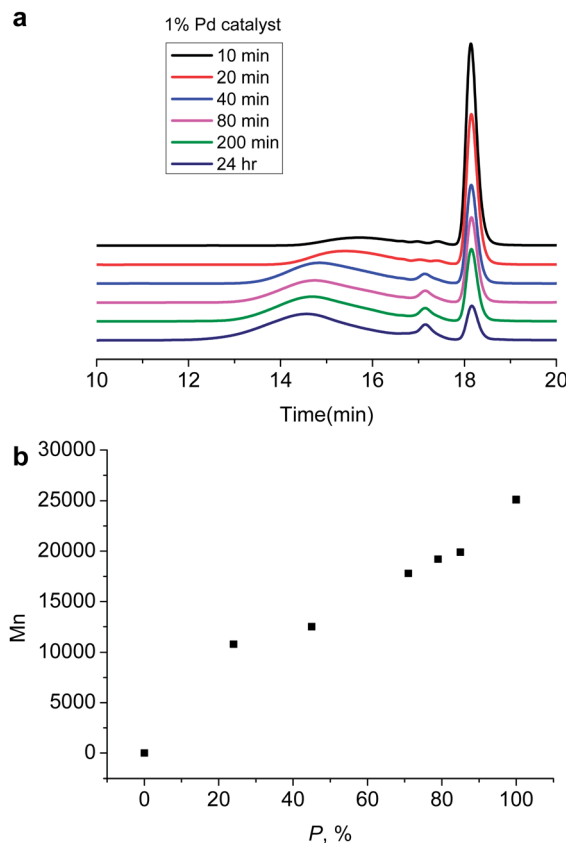
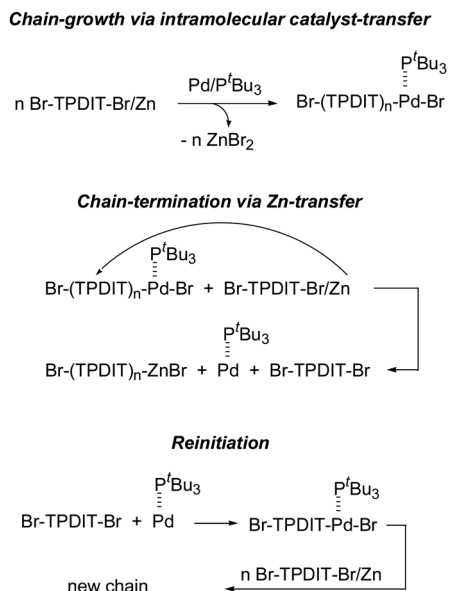


**Fig. 2** GPC elution curves of crude polymerization mixtures (a) and  $M_n$  ( $\text{g mol}^{-1}$ ) versus monomer conversion ( $P$ ) plot (b) for polymerization performed at  $[\text{Br-TPDIT-Br/Zn}]/[\text{Pd/P}^t\text{Bu}_3]$  ratio of 100/1.

at room temperature led to the formation of a dark-blue polymer within several hours (for UV-vis absorption spectrum, see Fig. S2, ESI†). Polymerization course was monitored at  $[\text{Br-TPDIT-Br/Zn}]/[\text{Pd/P}^t\text{Bu}_3]$  ratios of 50/1 and 100/1 (Table S1, ESI†). As seen from GPC of crude reaction mixtures (Fig. 2a), the peak corresponding to polymeric products increases while the monomer peak decreases upon increase of the polymerization time. Peaks which may correspond to oligomeric products (between the monomeric and polymeric peaks) are much smaller for all polymerization times. Such behavior is characteristic to the chain-growth propagation mechanism (*i.e.*, one-by-one addition of monomer molecules to growing chains) rather than step-growth propagation for which the monomer should be consumed early during polymerization. It is noteworthy that the molecular weight of the resulting PPDIT2 increases only modestly with the monomer consumption, presumably due to chain-termination reactions which limit the molecular weight at the  $M_n \approx 25 \text{ kg mol}^{-1}$ ,  $M_w \approx 45 \text{ kg mol}^{-1}$  level (Table S1†).

It is, however, obvious that this polymerization is far from being living (controlled) although it follows the chain-growth mechanism. Indeed, in living polymerization reactions, every initiator species polymerize one chain so that the formation of PPDIT2 with degree of polymerization ( $\text{DP}$ ) = 50 and 100 is expected for the monomer/catalyst ratios of 50/1 and 100/1,



Scheme 2 Plausible mechanisms of chain-propagation, -termination and -reinitiation processes occurred upon Pd/P<sup>t</sup>Bu-catalyzed polymerization of Br-TPDIT-Br/Zn.

respectively, instead of observed DP  $\approx$  25 for both catalyst loadings. In addition, the polydispersity index (PDI =  $M_w/M_n$ ) is relatively large and it increases with the monomer conversion increase,  $P$  (PDI = 1.5 for  $P$  = 24%; PDI = 1.8 for  $P$  = 85%). Similar limitation of the polymer molecular weight was earlier observed in catalyst-transfer polycondensation reactions of fluorene-based monomers. A possible reason for the observed chain-limitation phenomena is given in Scheme 2. The data suggest that up to DP  $\approx$  25, polymerization of Br-TPDIT-Br/Zn proceeds as one-by-one addition of monomers to propagating chains Br-(Ar)<sub>*n*</sub>-Pd(P<sup>t</sup>Bu<sub>3</sub>)-Br as it usually occurs in chain-growth catalyst-transfer polycondensation reactions (Scheme 2A).

At this stage, the catalytic cycle involves intramolecular transfer followed by intramolecular oxidative addition (OA) of a Pd(0) species to the C-Br bond, which is present at the end of the same polymerizing chain. It is noteworthy that the intermolecular transfer (diffusion) of the Pd(0) species followed by their intermolecular OA into the C-Br bond of the monomer does not occur at this polymerization stage (as follows from a coexistence during the polymerization of relatively high molecular weight PPDIT2 and unreacted monomer). This can be explained by (i) the intrinsic propensity of Pd(0) to form  $\pi$ -complexes making the intramolecular transfer to be an entropically more favored process; (ii) zinc organic monomer molecules are relatively electron-rich species which impedes the oxidative addition of Pd(0) to the C-Br bond of the monomer Br-TPDIT-Br/Zn. The situation changes when relatively large Br-(TPDIT)<sub>*n*</sub>-Pd(P<sup>t</sup>Bu<sub>3</sub>)-Br chains with DP  $\approx$  25 are formed. We suggest that for larger chains, a Zn-exchange reaction between the monomer and propagating chains takes place and it is responsible for the chain-transfer process (Scheme 2B). As reported previously, Br-TPDIT-Br/Zn is a charge-transfer complex in which the Zn atom is associated with Br-TPDIT-Br by

means of relatively weak donor-acceptor interactions. On the other hand, Br-(TPDIT)<sub>*n*</sub>-Pd(P<sup>t</sup>Bu<sub>3</sub>)-Br chains formed in the first polymerization stage contain many electron-deficient TPDIT repeat units which potentially form complexes with Zn atoms. Transfer of Zn from Br-TPDIT-Br/Zn to Br-(TPDIT)<sub>*n*</sub>-Pd(P<sup>t</sup>Bu<sub>3</sub>)-Br should reduce Pd(II) to Pd(0) to form PdP<sup>t</sup>Bu<sub>3</sub>, Br-(TPDIT)<sub>*n*</sub>-ZnBr and Br-TPDIT-Br. The intermolecular oxidative addition of free PdP<sup>t</sup>Bu<sub>3</sub> to the C-Br bond of Br-TPDIT-Br results in Br-TPDIT-Pd(P<sup>t</sup>Bu<sub>3</sub>)-Br which initiate a new chain. However, it remains unclear why the Zn-transfer process from Br-TPDIT-Br/Zn occurs preferentially with PPDIT2 chains having DP > 25 but not with shorter oligomers.

It should also be noted that although high molecular weight PTPDIT is not formed by the method developed herein, traditional step-growth polymerization methods provide PDI-based polymers with even lower molecular weights. Thus, PDI polymers with  $M_w$  in the 10–20 kg mol<sup>-1</sup> range were prepared by Hashimoto *et al.* by Stille and Suzuki polycondensation reactions.<sup>4</sup> Facchetti *et al.* reported Stille-based synthesis of P(PDI2OD-T2) (analogue of our PTPDIT) with a  $M_w$  of 32 kg mol<sup>-1</sup>, although the same polymerization method afforded much higher polymers in the case of structurally similar naphthalenediimide-based polymers.<sup>12b</sup> As such, the method developed herein is a viable alternative to conventional polycondensation schemes as it provides polymers with slightly higher molecular weights than previously reported methods.

### Field-effect transistor and photovoltaic characterization

Performance of PPDIT2 synthesized by the newly developed chain-growth method was further tested and compared with the performance of the same polymer obtained by traditional step-growth Stille coupling polycondensation (designated as PPDIT2<sub>control</sub>). It was previously demonstrated that this polymer exhibits typical n-type semiconductor behavior and provides an electron mobility of  $\sim 10^{-3}$  cm<sup>2</sup> V<sup>-1</sup> s<sup>-1</sup> when measured under ambient conditions. Typical output and transfer characteristics for transistors prepared from 8 g L<sup>-1</sup> solution of PPDIT2 in DCB (dichlorobenzene) are shown in Fig. 3. The n-type FET shows a saturated mobility of  $5 \times 10^{-3}$  cm<sup>2</sup> V<sup>-1</sup> s<sup>-1</sup>. This is a slightly higher mobility value than that previously reported for the polymer prepared by step-growth polymerization.

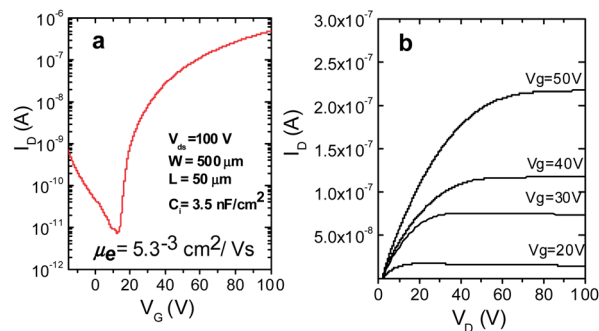


Fig. 3 Representative output (a) and transfer (b) characteristics of OFETs made using PPDIT2 prepared in this work ( $M_n$  = 15 kg mol<sup>-1</sup>, PDI = 1.8).

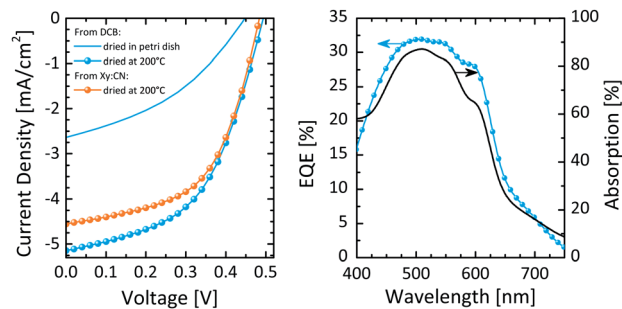


Fig. 4 (left) Current density–voltage characteristics under AM 1.5G illumination at  $100 \text{ mW cm}^{-2}$  of inverted solar cells prepared from a 1.5 : 1 mixture of P3HT and PPDIT2. Blends prepared from Xy : CN were dried at  $200 \text{ }^\circ\text{C}$  (orange spheres), while DCB-cast blends were either slowly dried in a Petri dish at room temperature (solid blue line) or fast dried at  $200 \text{ }^\circ\text{C}$  (blue spheres). (right) External quantum efficiency (EQE, blue spheres) of the  $200 \text{ }^\circ\text{C}$  dried, DCB-cast solar cell. Also shown is the active layer absorption (black line).

Photovoltaic performance of PPDIT2 was further tested and compared with the performance of PPDIT2<sub>control</sub>. PPDIT2 was used as the electron-accepting component, while regioregular P3HT served as an electron donor. Two solvent systems were explored in order to optimize the devices. The first system is a 1 : 1 solvent mixture of Xy (xylene) and the high boiling point solvent CN (chloronaphthalene), which was recently used to optimize blends of P3HT and P(NDI2OD-T2), the naphthalene diimide-based analogue polymer to PPDIT2 that is investigated here.<sup>34</sup> The preparation of the active layer includes a high-temperature drying step of the wet films directly after spin-coating. In the second recipe DCB was used as a solvent, which has shown to be an appropriate solvent for blends of P3HT and PPDIT2.<sup>35</sup> Solar cells were built in the inverted device configuration with a solution-processed electron-extracting zinc oxide bottom contact and a hole-extracting molybdenum trioxide top contact (for details see below). In accordance with the former results, we find that the inverted device structure behaves significantly better than the normal configuration, which has been assigned to the strong vertical composition gradient formed in P3HT:PPDIT2 blends.<sup>35</sup>

Fig. 4 displays the current density–voltage characteristics of PPDIT2-based solar cells under illumination with simulated sunlight. The devices show comparable characteristics when the active layer is dried at high temperature, while the cells prepared from DCB show a slightly higher short circuit current density ( $J_{\text{SC}}$ ) than those cast from the Xy : CN mixture. We obtain a maximum power conversion efficiency (PCE) of 1.3%. On the other hand, slow drying under DCB vapor results in a

drastic decrease in the  $J_{\text{SC}}$  and overall performance, similar to what was observed for P3HT:P(NDI2OD-T2) blends.<sup>34</sup>

For the best performing cell the external quantum efficiency (EQE) is also displayed in Fig. 4. The spectra reach a maximum of 32%, 50% higher than the best solar cells prepared from the naphthalene diimide-derivative. Also shown is the active layer absorption, which is calculated from the measured optical density of the blend. To account for the reflectance at the top electrode, we assumed that light passes the active layer two times. The similarity between absorption and EQE demonstrates that both polymers contribute equally to the photocurrent.

The performance of the PPDIT2 copolymer was further tested against the PPDIT2<sub>control</sub> copolymer, which was synthesized by standard step-growth polycondensation.<sup>2</sup> The solar cell parameters are given in Table 1. Compared to the best performing device in Fig. 4, the PPDIT2<sub>control</sub>-based device shows a lower  $J_{\text{SC}}$  but a higher fill factor and open circuit voltage, which results in an overall similar PCE of 1.4%. We note that in contrast to PPDIT2<sub>control</sub>-prepared solar cells, PPDIT2-based devices were not fully optimized, as the subject of this paper is to provide the proof of principle rather than performing a detailed analysis and optimization of the solar cell performance. Nevertheless, we conclude that the performance of the PPDIT2 copolymer is comparable, whether it was synthesized by a step-growth or chain-growth method. This demonstrates that the newly designed method produces polymers with high performance, which can be readily applied in functional devices.

## Conclusion

Herein, we report the chain-growth polymerization method to synthesize perylene diimide-based conjugated polymers suitable for solar cell and transistor applications. Ni-catalysts previously used for chain-growth polymerization of the naphthalene-diimide monomer were inactive to the polymerization of perylene diimide-based monomers. However, the palladium complex ligated by bulky electron-rich tri-*tert*-butylphosphine was found to be an appropriate catalyst to enable the chain-growth polymerization of Br-TPDIT-Br/Zn to PPDIT2 with moderate molecular weight and moderate polydispersity. This is the second example of the polymerization of unusual anion-radical aromatic complexes formed in a reaction of active Zn and electron-deficient diimide-based aryl halides. As such, the discovered polymerization is not a specific reactivity feature of the naphthalene-diimide derivatives<sup>26</sup> but displays a rather general polymerization tool. This is an important finding, given

Table 1 Solar cell parameters for the devices discussed in the text

Blend	Solvent	Drying	$J_{\text{SC}}$ [ $\text{mA cm}^{-2}$ ]	FF [%]	$V_{\text{OC}}$	PCE [%]
P3HT:PPDIT2	DCB	$25 \text{ }^\circ\text{C}$ (Petri dish)	2.64	39	0.45	0.5
P3HT:PPDIT2	DCB	$200 \text{ }^\circ\text{C}$	5.14	51	0.49	1.3
P3HT:PPDIT2	1 : 1 Xy : CN	$200 \text{ }^\circ\text{C}$	4.55	55	0.48	1.2
P3HT:PPDIT2 <sub>control</sub>	1 : 1 Xy : CN	$200 \text{ }^\circ\text{C}$	4.37	61	0.53	1.4



the significantly higher maximum external quantum efficiency that can be reached with PDI-based materials (32–45%)<sup>4,35</sup> in all-polymer solar cells compared to NDI-based copolymers (15–30%).<sup>36,37</sup> Our studies revealed that PPDIT2 synthesized by the new method and the previously published polymer prepared by step-growth Stille polycondensation show similar electron mobility and all-polymer solar cell performance. However, the polymerization reported herein has several technological advantages as it proceeds relatively fast at room temperature and does not involve toxic tin-based compounds. Because chain-growth polymerization reactions are generally well-suited for preparation of well-defined multi-functional polymer architectures, the next target is to explore the utility of the discovered polymerization in the synthesis of end-functionalized polymers and block copolymers. Such materials would be helpful in better controlling the nanoscale morphology of polymer blends in all-polymer solar cells.

## Acknowledgements

AK and MS gratefully acknowledge support from the German Excellence Initiative *via* the Cluster of Excellence EXC 1056 “Center for Advancing Electronics Dresden” (cFAED) and DFG (SPP 1355) “Elementary Processes of Organic Photovoltaics”.

## Notes and references

- 1 A. Facchetti, *Chem. Mater.*, 2011, **23**, 733.
- 2 (a) X. Zhan, Z. Tan, B. An, Z. Domercq, X. Zhang, S. Barlow, Y. Li, D. Zhu, B. Kippelen and S. R. Marder, *J. Am. Chem. Soc.*, 2007, **129**, 7246; (b) Z. Chen, Y. Zheng, H. Yan and A. Facchetti, *J. Am. Chem. Soc.*, 2009, **131**, 8.
- 3 E. Kozma and M. Catellani, *Dyes Pigment.*, 2013, **98**, 160.
- 4 E. Zhou, J. Cong, Q. Wei, K. Tajima, C. Yang and K. Hashimoto, *Angew. Chem.*, 2011, **50**, 2799.
- 5 A. Facchetti, *Mater. Today*, 2013, **16**, 123.
- 6 T. Earmme, Y.-J. Hwang, N. M. Murari, S. Subramaniyan and S. A. Jenekhe, *J. Am. Chem. Soc.*, 2013, **135**, 14960–14963.
- 7 Z. He, C. Zhong, X. Huang, W.-Y. Wong, H. Wu, L. Chen, S. Su and Y. Cao, *Adv. Mater.*, 2011, **23**, 4636–4643.
- 8 Y. Yi, V. Coropceanu and J.-L. Brédas, *J. Mater. Chem.*, 2011, **21**, 1479.
- 9 C. R. McNeill, B. Watts, L. Thomsen, W. J. Belcher, N. C. Greenham and P. C. Dastoor, *Nano Lett.*, 2006, **6**, 1202.
- 10 D. Mori, H. Benten, H. Ohkita, S. Ito and K. Miyake, *ACS Appl. Mater. Interfaces*, 2012, **4**, 3325.
- 11 K. Nakabayashi and H. Mori, *Macromolecules*, 2012, **45**, 9618; K. Johnson, Y.-S. Huang, S. Huettner, M. Sommer, M. Brinkmann, R. Mulherin, D. Niedzialek, D. Beljonne, J. Clark, W. T. S. Huck and R. H. Friend, *J. Am. Chem. Soc.*, 2013, **135**, 5074.
- 12 (a) H. Yan, Z. Chen, Y. Zheng, C. Newman, J. R. Quinn, F. Dötz, M. Kastler and A. Facchetti, *Nature*, 2009, **457**, 679; (b) Z. Chen, Y. Zheng, H. Yan and A. Facchetti, *J. Am. Chem. Soc.*, 2009, **131**, 8.
- 13 M. J. Robb, D. Montarnal, N. D. Eisenmenger, S.-Y. Ku, M. L. Chabynyc and C. J. Hawker, *Macromolecules*, 2013, **46**, 6431.
- 14 U. Scherf, A. Gutacker and N. Koenen, *Acc. Chem. Res.*, 2008, **41**, 1086; S.-Y. Ku, M. A. Brady, N. D. Treat, J. E. Cochran, M. J. Robb, E. J. Kramer, M. L. Chabynyc and C. J. Hawker, *J. Am. Chem. Soc.*, 2012, **134**, 16040.
- 15 M. Szwarc, *Nature*, 1956, **178**, 1168.
- 16 B. Carsten, F. He, H. J. Son, T. Xu and L. Yu, *Chem. Rev.*, 2011, **111**, 1493.
- 17 I. Osaka and R. D. McCullough, *Acc. Chem. Res.*, 2008, **41**, 1202.
- 18 T. Yokozawa and A. Yokoyama, *Chem. Rev.*, 2009, **109**, 5595.
- 19 Y. H. Geng, L. Huang, S. P. Wu and F. S. Wang, *Sci. China: Chem.*, 2010, **53**, 1620.
- 20 (a) A. Kiriy, V. Senkovskyy and M. Sommer, *Macromol. Rapid Commun.*, 2011, **32**, 1503; (b) R. Tkachov, V. Senkovskyy, H. Komber and A. Kiriy, *Macromolecules*, 2011, **44**, 2006.
- 21 K. Okamoto and C. K. Luscombe, *Polym. Chem.*, 2011, **2**, 2424.
- 22 N. Marshall, S. K. Sontag and J. Locklin, *Chem. Commun.*, 2011, **47**, 5681.
- 23 E. L. Lanni and A. J. McNeil, *J. Am. Chem. Soc.*, 2009, **131**, 16573.
- 24 E. Elmaleh, A. Kiriy and W. T. S. Huck, *Macromolecules*, 2011, **44**, 9057.
- 25 H. Komber, V. Senkovskyy, R. Tkachov, K. Johnson, A. Kiriy, W. T. S. Huck and M. Sommer, *Macromolecules*, 2011, **44**, 9164.
- 26 V. Senkovskyy, R. Tkachov, H. Komber, M. Sommer, M. Heuken, B. Voit, W. T. S. Huck, V. Kataev, A. Petr and A. Kiriy, *J. Am. Chem. Soc.*, 2011, **131**, 19966.
- 27 V. Senkovskyy, R. Tkachov, H. Komber, A. John, J.-U. Sommer and A. Kiriy, *Macromolecules*, 2012, **5**, 7770.
- 28 E. Wang, Z. Ma, Z. Zhang, K. Vandewal, P. Henriksson, O. Inganäs, F. Zhang and M. R. Andersson, *J. Am. Chem. Soc.*, 2011, **133**, 14244.
- 29 R. Stalder, J. Mei and J. R. Reynolds, *Macromolecules*, 2010, **43**, 8348.
- 30 J. Li, Y. Zhao, H. S. Tan, Y. Guo, C.-A. Di, G. Yu, Y. Liu, M. Lin, S. H. Lim, Y. Zhou, H. Su and B. S. Ong, *Sci. Rep.*, 2012, **2**, 754.
- 31 L. Shi, Y. Y. Chu, P. Knochel and H. Mayr, *Org. Lett.*, 2009, **11**, 3502.
- 32 (a) C. Dai and G. C. Fu, *J. Am. Chem. Soc.*, 2001, **123**, 2719; (b) G. C. Fu, *Acc. Chem. Res.*, 2008, **41**, 1555–1564; (c) M. R. Biscoe, T. E. Barder and S. L. Buchwald, *Angew. Chem., Int. Ed.*, 2007, **46**, 7232.
- 33 A. Yokoyama, H. Suzuki, Y. Kubota, K. Ohuchi, H. Higashimura and T. Yokozawa, *J. Am. Chem. Soc.*, 2007, **129**, 7236; T. Beryozkina, K. Boyko, N. Khanduyeva, V. Senkovskyy, M. Horecha, U. Oertel, F. Simon, M. Stamm and A. Kiriy, *Angew. Chem., Int. Ed.*, 2009, **48**, 2695; S. Kang, R. J. Ono and C. W. Bielawski, *J. Am. Chem. Soc.*, 2013, **135**, 4984.

- 34 M. Schubert, D. Dolfen, J. Frisch, S. Roland, R. Steyrlleuthner, B. Stiller, Z. Chen, U. Scherf, N. Koch, A. Facchetti and D. Neher, *Adv. Energy Mater.*, 2012, **2**, 369.
- 35 Y. Zhou, Q. Yan, Y.-Q. Zheng, J.-Y. Wang, D. Zhao and J. Pei, *J. Mater. Chem. A*, 2013, **1**, 6609.
- 36 E. Zhou, J. Cong, M. Zhao, L. Zhang, K. Hashimoto and K. Tajima, *Chem. Commun.*, 2012, **48**, 5283.
- 37 Y.-J. Hwang, G. Ren, N. M. Murari and S. A. Jenekhe, *Macromolecules*, 2012, **45**, 9056.
- 38 Y. Sun, J. H. Seo, C. J. Takacs, J. Seifert and A. J. Heeger, *Adv. Mater.*, 2011, **23**, 1679.